ISSN 2229-5518

Static stability of a Rotating Symmetric Sandwich beam subjected to axial pulsating load

[1]Madhumita Mohanty, [2]Madhusmita Pradhan
[1]KIIT Deemed to be University, BBSR, madhumita.mohanty92@gmail.com
[2]VSSUT, Burla, osme.madhusmita@gmail.com

Abstract— the static stability of a rotating symmetric sandwich beam subjected to axial pulsating load is studied under two different boundary conditions. The non dimensional equation of motion and boundary conditions are derived using Hamilton's principle. A set of Hill's equation with complex coefficient are derived using Galerkin's method. The effect of core loss factor, hub radius, Shear modulus, angular velocity of beam, rotation parameter and ratio of width of elastic layers of beam on static buckling load of the system is investigated through a series of graph using required MATLAB program.

Index Terms— Static stability, Rotaing Sandwich beam, Pulsating Load, Static buckling load, Coreloss factor, Rotation parameter.

1 INTRODUCTION

Vibration control of machine componets are important area of study to secure the mechanical system. Use of Sandwich structures is very much popular because of its light weight, high strength, high modulus and high stiffness to weight ratio. The sandwich structures being used as rotor blades, turbine blades in aircrafts and robot arms in other applications can be modeled as rotating beams under different boundary conditions. In practical application the sandwich structures are exposed to time varying loads, the system experiences parametric instability.

1.1 LIST OF SYMBOLS

G_2^* : $G_2(1+jn)$, complex shear modulus of core

g^* : g(1+jn), complex shear parameter, g : Shear parameter

b : Distance of the nearer end of the beam from the axis of rotation(hub radius), $\bar{b}$: $\dfrac{b}{l}$, γ_2 : Shear strain in the core

h_{31} : $(h_3)/(h_1)$, h_{21} : $(h_2)/(h_1)$

l : Beam length, lh_1 : l/h_1

$\bar{m}$: Mass/unit length of beam

λ_0, λ_1 : Rotation parameter

Ω_0 : Uniform angular velocity of the beam about Z axis

α : $\dfrac{E_1A_1}{E_3A_3}$, E_{31} : $\dfrac{E_3}{E_1}$, $\bar{w}$: $\dfrac{w}{l}$

ω : Frequency of forcing function, $\bar{\omega}$: Non-dimensional forcing frequency

$\bar{P}_1$: Non dimensional amplitude for the dynamic loading

B : Width of beam, ρ_i : Density of ith layer

1.1 OBJECTIVE

The main objective of the study is to investigate the static staility of a symmetric rotating sandwich beam subjected to axial pulsating load for two different boundary conditions viz Pinned-Pinned and Guided- Pinned. Combining the Hamilton's energy principle and Galerkin's method a set of Hill's equation is derived for the considered system. The static buckling load is determined. Numerical computation and graphical representation is done using required MATLAB code. The stability analysis is done by considering the hub radius, shear parameter, rotation parameter, angular velocity of beam, coreloss factor and ratio of thickness of elastic layers.

2 LITERATURE REVIEW

The study of sandwich structures has attended a great practical importance from economical point of view as well as for effective vibration control. Ghosh et al [10] studied the dynamic stability of viscoelastically supported sandwich beams. Dash et al [9] investigated the dynamic stability of an asymmetric sandwich beam resting on Pasternak foundation. Nayak et al [5] analyzed the static stability of viscoelastically supported asymmetric sandwich beam with thermalgradient. Pradhan et al [8] analyzed the static and dynamic stability of asymmetric sandwich beam resting on a variable Pasternak foundation. Pradhan et al [2] studied the dynamic stability of of an asymmetric rotating sandwich beam subjected to thermal gradient.

From the available literature it has been observed that no work has been done on stability of symmetric rotating sandwich beam subjected to axial pulsating load. So in this analysis the static stability of a symmetric rotating sandwich beam is done for two different boundary conditions viz Pinned-Pinned and Clamped-Pinned.

3 Problem Formulation

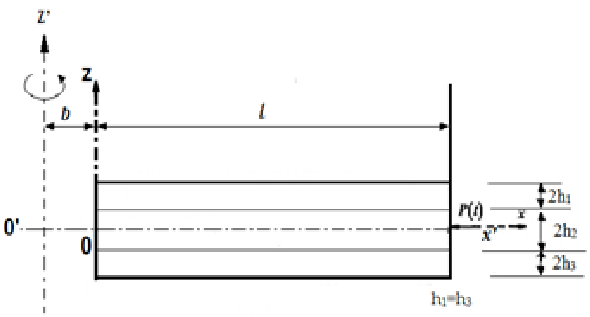

Fig 1: System Configuration

The equation of motion is derived by considering the following assumptions:

- The beam transverse deflection is small and is same everywhere in a given cross section.
- The elastic layer obeys Euler-Bernoulli assumption of beam theory.
- The layers are perfectly bonded so that displacements are continuous across the interfaces.
- Bending and the extensional effects in the core are negligible.
- Rotary inertia effects in layers are negligible.
- Damping in the core is predominantly due to shear.
- Kerwin's assumption is used as force resultant in the middle visco-elastic layer is neglected as Young's modulus is very small compared to the module of outer two layers. So $E_1 A_1 U_{1,x} + E_3 A_3 U_{3,x} = 0$

The expression for potential energy (v), kinetic energy (T) and work done (w_p) for given system are as follows:

$$V = \frac{1}{2}\int_0^l E_1 A_1 U_{1,x}^2 dx + \frac{1}{2}\int_0^l E_3 A_3 U_{3,x}^2 dx + \frac{1}{2}\int_0^l (E_1 I_1 + E_3 I_3) w_{xx}^2 dx + \frac{1}{2} G_2^* \int_0^l A_{2,x} \gamma_2^2 dx$$

$$T = \frac{1}{2}\int_0^l m w_t^2 dx + \frac{1}{2}\Omega_0^2 \int_0^l [m(b+x)\int_0^x w_x^2 dx] dx + \frac{1}{2}\int_0^l m\Omega_0^2 w^2 dx$$

$$w_p = \frac{1}{2}\int_0^l p(t) w_x^2 dx$$

Where U_1 and U_3 are the displacements in the top and bottom layers, $w_x = \frac{\partial w}{\partial x}, w_t = \frac{\partial w}{\partial t}$ and γ_2 is the shear strain in the middle layer given by $\gamma_2 = \frac{U_1 - U_3}{2h_2} - \frac{Cw_x}{2h_2}$. U_3 is eliminated by using the Kerwin's assumption.

The application of Hamilton's principle, $\delta\int_{t_1}^{t_2} (T - V + w_p) dt = 0$ leads to the following non-dimensional equations of motion.

$$\bar{m}\bar{w}_{\bar{t}\bar{t}} + [1 + \frac{\lambda_0^2}{(lh_1)^2}\{\frac{f}{l^2} - (\bar{x}+\bar{b})^2\}]\bar{w}_{\bar{x}\bar{x}\bar{x}\bar{x}} - \frac{2\lambda_0^2}{(lh_1)^2}(\bar{x}+\bar{b})\bar{w}_{\bar{x}\bar{x}\bar{x}} + [\frac{\lambda_0^2}{(lh_1)^2} - \lambda_0^2\{\frac{f}{l^2} - (\bar{x}+\bar{b})^2\} - 3g^*(1+\frac{h_{12}+h_{32}}{2})^2 + \bar{p}(\bar{t})]\bar{w}_{\bar{x}\bar{x}} + \lambda_0^2(\bar{x}+\bar{b})\bar{w}_{\bar{x}} + \frac{3}{2}g^* lh_1 h_{12}(1+\frac{h_{12}+h_{32}}{2})(1+\alpha)\frac{2(h_2)}{C}\gamma_{2,\bar{x}} = 0 \quad (1)$$

$$\frac{2(h_2)}{C}\gamma_{2,\bar{x}\bar{x}} - \frac{g}{4}h_{12}^2(\frac{1+E_{31}}{1+\alpha^2 E_{31}})(1+\alpha)[(1+\alpha)\frac{2(h_2)}{C}\gamma_2 - (\frac{2(1+((h_{12}+h_{32})/2))}{(lh_{10}h_{12})})\bar{w}_{\bar{x}}] = 0 \quad (2)$$

In the above:

$$\bar{w}_{\bar{x}\bar{x}\bar{x}\bar{x}} = \frac{\partial^4 \bar{w}}{\partial \bar{x}^4}, \bar{w}_{\bar{x}\bar{x}} = \frac{\partial^2 \bar{w}}{\partial \bar{x}^2}, \gamma_{2,\bar{x}\bar{x}\bar{x}} = \frac{\partial^3 \gamma_2}{\partial \bar{x}^3}, \gamma_{2,\bar{x}\bar{x}} = \frac{\partial^2 \gamma_2}{\partial \bar{x}^2},$$

$$\bar{x} = \frac{x}{l}, \bar{U} = \frac{U}{l}, \bar{w} = \frac{w}{l}, \bar{t} = \frac{t}{t_0}, C = (h_1) + (2h_2) + (h_3)$$

$$t_0 = [\frac{\rho_1 A_1 l^4}{E_1 I_1}]^{\frac{1}{2}}, \bar{P_0} = \frac{P_0 l^2}{E_1 I_1}, \bar{P_1} = \frac{P_1 l^2}{E_1 I_1}, \bar{P} = \bar{P_0} + \bar{P_1}\cos(\bar{w}\bar{t}),$$

$$\bar{\omega} = \omega t_0, g^* = \frac{G_2^* h_{21}(lh_1)^2}{E_1(1+E_{31})}$$

The associated boundary condition at $\bar{x} = 0$ and $\bar{x} = 1$ are:

$$[1 + \frac{\lambda_0^2(1+E_{31})}{(lh_1)^2(E_{31})}\{\frac{f}{l^2} - (\bar{x}+\bar{b})^2\}]\bar{w}_{\bar{x}\bar{x}\bar{x}} - \frac{2\lambda_0^2(1+E_{31})}{(lh_1)^2(1+E_{31})}(\bar{x}+\bar{b})\bar{w}_{\bar{x}\bar{x}} = 0 \quad (3)$$

or $\bar{w}_{\bar{x}} = 0$ (4)

$$[\frac{\lambda_0^2(1+E_{31})}{(lh_1)^2(1+E_{31})} - \lambda_0^2\{\frac{f}{l^2} - (\bar{x}+\bar{b})^2\} - 3g^*(1+\frac{h_{12}+h_{32}}{2})^2 + \bar{p}(\bar{t})]\bar{w}_{\bar{x}} = 0 \quad (5)$$

or $\bar{w} = 0$ (6)

$$\frac{3}{2}g^* lh_1 h_{12}(1+\frac{h_{12}+h_{32}}{2})(1+\alpha)\frac{2(h_2)}{C}\gamma_{2,\bar{x}} = 0 \quad (7)$$

or $\gamma_2 = 0$ (8)

APPROXIMATE SOLUTION:

Solution of equation (1) and (2) are assumed in the form

$$\bar{w}(\bar{x},\bar{t}) = \sum_{i=1}^{i=p} w_i(\bar{x}) f_i(\bar{t}) \quad (9)$$

$$\bar{\gamma}_2(\bar{x},\bar{t}) = \sum_{k=p+1}^{k=2p} \gamma_k(\bar{x}) f_k(\bar{t}) \quad (10)$$

Here w_i and γ_k are the shape functions and f_i and f_k are the generalized coordinates. w_i and γ_k are to be chosen to satisfy as many boundary conditions as possible.

For Pinned-Pinned (P-P) case

$w_i(\bar{x}) = \sin(i\pi\bar{x})$, $\gamma_k(\bar{x}) = \cos(k\pi\bar{x})$

For clamped-pinned (C-P) case

$$w_i(\bar{x}) = 2(i+2)\bar{x}^{(i+1)} - (4i+6)\bar{x}^{(i+2)} + 2(i+1)\bar{x}^{(i+3)}$$

$$\gamma_{\bar{k}}(\bar{x}) = (\bar{k}+1)\bar{x}^{\bar{k}} - \bar{k}\bar{x}^{(\bar{k}+1)}$$

Where $\bar{k} = k - p$

Substituting above values in (1) and (2) and use of the general Galerkin method yields the following matrix equations of motion in the generalized coordinates.

$$[m]\{\ddot{Q}_1\} + [k_{11}]\{Q_1\} + [k_{12}]\{Q_2\} = \{0\} \qquad (11)$$

$$[k_{21}]\{Q_1\} + [k_{22}]\{Q_2\} = \{0\} \qquad (12)$$

Where, $\{Q_1\} = \{f_1, \ldots\ldots\ldots\ldots, f_p\}^T$ (13)

$$\{Q_2\} = \{f_{p+1}, \ldots\ldots\ldots\ldots, f_{2p}\}^T \qquad (14)$$

$$m_{ij} = \int_0^1 \bar{m} w_i w_j d\bar{x} \qquad (15)$$

$$k_{11ij} = \int_0^1 [1+\lambda_1\{\frac{f}{l^2} - (\bar{x}+\bar{b})^2\}] w_i'' w_j'' d\bar{x} + \lambda_0^2 \int_0^1 \{\frac{f}{l^2} - (\bar{x}+\bar{b})^2\} w_i' w_j' d\bar{x} + \{3g^*(1+\frac{h_{12}+h_{32}}{2})^2 - \bar{p}(\bar{t})\} \int_0^1 w_i' w_j' d\bar{x} \qquad (16)$$

$$k_{12ij} = -(\frac{3}{2}) g^* l h_1 h_{12} (1+\alpha)(1+\frac{h_{12}+h_{32}}{2})(\int_0^1 u_l w_i' d\bar{x}) \qquad (17)$$

$$k_{22kl} = 3*(lh_1)^2 \frac{(1+\alpha^2 E_{31})}{(1+E_{31})}(\int_0^1 u_k' u_l' d\bar{x}) + \qquad (18)$$

$$\frac{3}{4} g^* (lh_1)^2 h_{12}^2 (1+\alpha)^2 (\int_0^1 u_k u_l d\bar{x})$$

In the above, $u_k = \frac{2h_2}{C}\gamma_k, u_l = \frac{2h_2}{C}\gamma_l$ and $w_i' = \frac{\partial w_i}{\partial x}$

$f = (l+b)^2$, for x=l

$= b^2$, for x=0

$= \frac{l^2}{3} + b^2 + bl$, for other cases

$$[k_{21}] = [k_{12}]^T$$

The equations (11) and (12) are further simplified to

$$[m]\{\ddot{Q}_1\} + [[k] - \bar{P}_0[H]]\{Q_1\} - \bar{P}_1 \cos(\bar{\omega} t)[H]\{Q_1\} = \{0\} \qquad (19)$$

Where, $[k] = [\bar{k}] - [k_{12}][k_{22}]^{-1}[k_{12}]^T$ (20)

$$H_{ij} = \int_0^1 w_i' w_j' d\bar{x} \qquad (21)$$

$$[\bar{k}]_{ij} = \int_0^1 [1+\lambda_1\{\frac{f}{l^2} - (\bar{x}+\bar{b})^2\}] w_i'' w_j'' d\bar{x} + \lambda_0^2 \int_0^1 \{\frac{f}{l^2} - (\bar{x}+\bar{b})^2\} w_i' w_j' d\bar{x} + \{3g^*(1+\frac{h_{12}+h_{32}}{2})^2\} \qquad (22)$$

$$\int_0^1 w_i' w_j^i d\bar{x}$$

4 NUMERICAL RESULTS AND DISCUSSION

Numercal results were obtained for various values of the parameters such as shear parameter, core loss factor, hub radius, rotation parameter, core density parameter, ratio of thickness of two elastic layers and presented graphically.

Figures 2 to 7 shows the effect of various parameters on the static bukling load.

: Pinned-Pinned
: clamped- Pinned

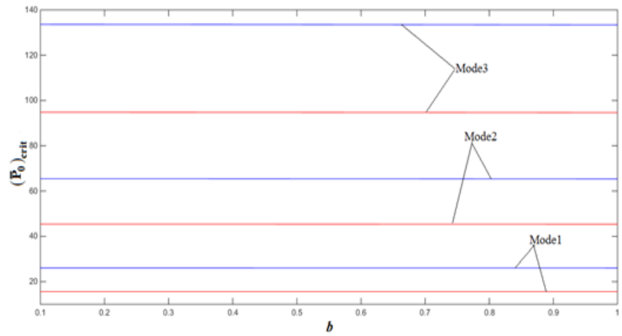

(Fig 2: Effect of hub radius on Static buckling load)

The effect of b on static buckling load is shown in fig 2. With increase in value of b, the static buckling load increases marginally for both boundary conditions.

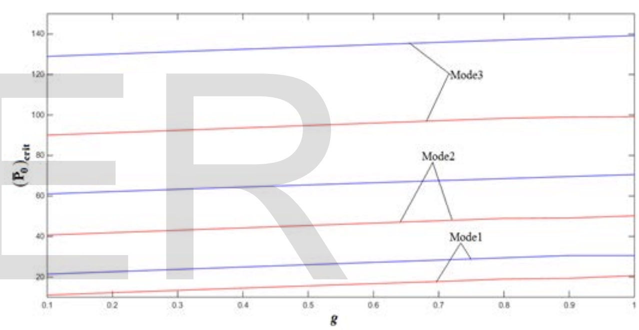

(Fig 3: Effect of g on static buckling load)

Figure 3 shows the effect of g on static buckling load of the system and it shows with increase in g the static buckling load of the system increases by increasing the stability of the system for both boundary conditions.

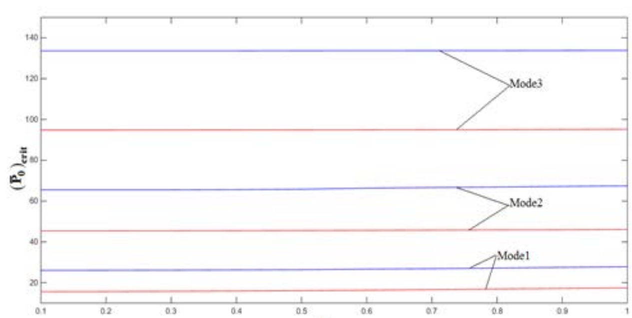

(Fig 4: Effect of η on static buckling load)

The effect of η on static buckling load of the system is shown in figure4. It shows that with increase in η, the static stability of the syatem increases marginally as the static buckling loads ncrease.

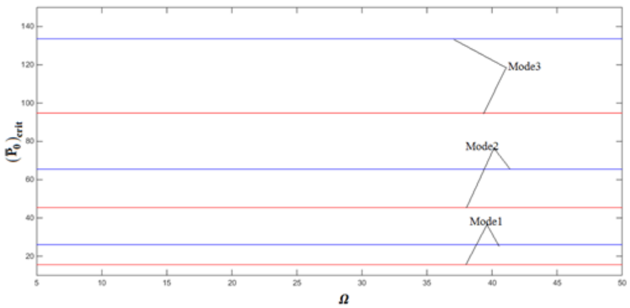

(Fig5: Effect of Ω on static buckling load)

Figure 5 shows the effect of angular velocity of beam (Ω) on static buckling load. It shows that with increase in angular velocity there is no change in static buckling load. Sothis property makes it suitable for high speed applcation.

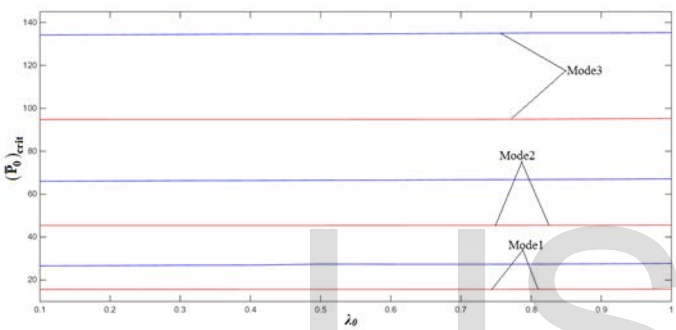

(Fig 6: Effect of λ_0 on static buckling load)

Figure6 shows the effect of λ_0 on static buckling load of the system. With increase in λ_0 the static buckling load increases by enhancing the static stability of the system.

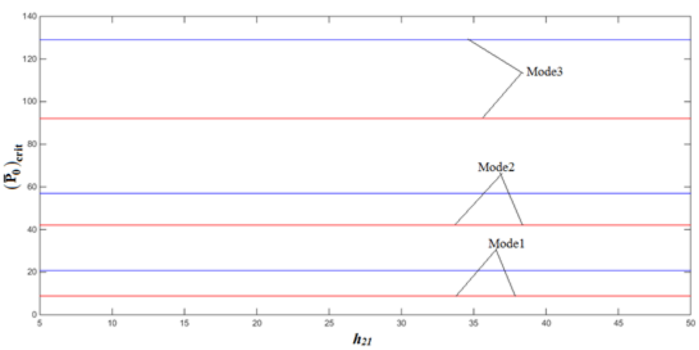

(Fig 7: Effect of h_{21} on static buckling load)

The effect of h_{21} on static buckling load of the system is depicted in figure figure7. It shows that with increase in of h_{21} the static stability of the system icreases by icreasing the static buckling load.

5 Conclusion

The static stability analysis of a symmetric rotating sandwich beam subjected to a axial pulsating load is investigated for Pinned-Pinned and Clamped-pinned boundary condition. The results obtained from the numerical analysis reveal that static stability of the system increases with increase with b, g, η, λ_0 and h_{21}. The static stability of the system is independent of the angular velocity of the system.

References

[1]M. Pradhan, M. K. Mishra, and P. R. Dash. "Stability analysis of an asymmetric tapered sandwich beam with thermal gradient." *Procedia Engineering* 144 (2016)

[2] Madhusmita Pradhan, Reeta Parida, and Pusparaj Dash. "Dynamic stability analysis of an asymmetric rotating sandwich beam subjected to thermal gradient." Proceedings of ICRAMM-2016, Paper no:CS04.

[3] Rajesh K Bhangale and N. Ganesan. "Thermoelastic buckling and vibration behavior of a functionally graded sandwich beam with constrained viscoelastic core." *Journal of Sound and Vibration* 295.1-2 (2006): 294-316.

[4] Bachir Bouderba et al. "Thermal stability of functionally graded sandwich plates using a simple shear deformation theory." *Structural Engineering and Mechanics* 58.3 (2016): 397-422.

[5]S. Nayak et al. "Static stability of a viscoelastically supported asymmetric sandwich beam with thermal gradient."*International Journal of Advanced Structural Engineering (IJASE)* 6.3 (2014): 65.

[6] S. K. Jalali, M. H. Naei and A. Poorsolhjouy. "Thermal stability analysis of circular functionally graded sandwich plates of variable thickness using pseudo-spectral method."*Materials & design* 31.10 (2010): 4755-4763.

[7] Chung-Yi Lin and Lien-Wen Chen. "Dynamic stability of a rotating beam with a constrained damping layer." Journal of sound and vibration 267.2 (2003): 209-225

[8]M. Pradhan, P. R. Dash, and P. K. Pradhan. "Static and dynamic stability analysis of an asymmetric sandwich beam resting on a variable Pasternak foundation subjected to thermal gradient." *Meccanica* 51.3 (2016): 725-739.

[9] P. R Dash, B. B. Maharathi and K. Ray. "Dynamic Stability of an Asymmetric Sandwich Beam Resting on a Paternak Foundation." *Journal of Aerospace Science and Technologies*62.1 (2010): 66.

[10] Ranajay Ghosh et al. "Dynamic stability of a viscoelastically supported sandwich beam." *Structural Engineering and Mechanics* 19.5 (2005): 503-517.

[11] Biswajit Nayak, Santosha K. Dwivedy, and K. S. R. K. Murthy. "Vibration analysis of a three-layer magnetorheological elastomer embedded sandwich beam with conductive skins using finite element method." Proceedings of the Institution of Mechanical Engineers, Part C: Journal of Mechanical Engineering Science 227.4 (2013): 714-729.

[12] Rahul E. Dhoble and R. B. Barjibhe. "Study on vibration analysis of sandwich cantilever beam using finite element ansys software." (2016).

[13]Obbineni, Mallikarjana reddy. "Dynamic Stability Analysis of Sandwich Beam with Functionally Graded Material Constraining Layer." *NIT, Rourkela, May* (2013).

[14] Saeid Shahedi, and Mehdi Mohammadimehr. "Nonlinear high-order dynamic stability of AL-foam flexible cored sandwich beam with variable mechanical properties and carbon nanotubes-reinforced composite face sheets in thermal environment." *Journal of Sandwich Structures & Materials*(2017)

[15] Vijay K. Goyal and Rakesh K. Kapania. "Dynamic stability of uncertain laminated beams subjected to subtangential loads." *International Journal of Solids and Structures* 45.10 (2008)